# Reconstructing Multibeam Echosounder Bathymetry with Generative Adversarial Networks: Toward Efficient Use of Survey Resources

Haitham Ezzy[1], Dror Angel[2], Anna Brook[1]

[1] Laboratory of Spectroscopy and Remote Sensing, School of Environmental Sciences, University of Haifa, Israel
[2] The Leon Recanati Institute for Maritime Studies, University of Haifa, Israel

**Keywords:** Bathymetry, Multibeam Echosounder. LiDAR, Super Resolution, Generative Adversarial Network, Image Reconstruction.

**Abstract**

The spatial accuracy and resolution of Multibeam Echosounder data are inherently lower than those of high-resolution underwater LiDAR measurements. However, while Multibeam Echosounder provides wide coverage and extensive historical availability, LiDAR is costly and covers relatively small areas. In this study, we propose an innovative approach to enhance Multibeam Echosounder resolution using a Super-Resolution Generative Adversarial Network with direct comparison to LiDAR data for accuracy assessment. The methodology involves converting Multibeam Echosounder data into grayscale format using various depth gradient techniques, analyzing differences in submarine geomorphology through calculations of slope and aspect, and evaluating statistical accuracy. The results show that the Super-Resolution Generative Adversarial Network model successfully improves Multibeam Echosounder resolution, producing data that closely correspond to LiDAR measurements, particularly in flat, sandy seabed areas. In contrast, regions with complex or rocky terrain exhibited more pronounced deviations, especially in aspect metrics, emphasizing the challenges associated with maintaining topographic orientation throughout the resolution enhancement process. The main conclusion is that enhancing Multibeam Echosounder data using Super-Resolution Generative Adversarial Network enables broader utilization of existing datasets to generate high-resolution models, offering a more cost-effective and accurate solution for seafloor mapping in areas where LiDAR data are unavailable.

## 1. Introduction

The evolution of the seabed is governed by a combination of interacting processes, including hydrodynamic forces (such as currents and waves), sediment transport mechanisms, and morphodynamic feedbacks(Wang et al., 2011). Mapping the ocean floor serves essential purposes in navigation, resource management, and scientific research; however, scientists face major challenges due to the ocean’s vast extent and limited underwater accessibility (NOAA Ocean Exploration, 2002; Wölfl et al., 2019). Globally, the seafloor remains largely unmapped at an acceptable resolution—only about 25% of the ocean floor has been documented, leaving approximately 75% of global bathymetry unexplored(Hornyak, 2024; Mayer et al., 2018).

Current satellite-altimetry–based representations of the seafloor achieve only kilometer-scale resolution, which fails to capture essential seabed features such as small ridges, seamounts, and slope breaks(Smith & Sandwell, 1997; Weatherall et al., 2015). Global initiatives such as Seabed 2030 aim to produce a comprehensive, high-resolution map of the entire seafloor by 2030 (Mayer et al., 2018; Wölfl et al., 2019), underscoring the urgent need for innovative methodologies to accelerate bathymetric data acquisition.

Multibeam Echosounder (MBES) systems represent the most accurate and detailed technology for detecting seabed features that single-beam sonar and historical lead-line soundings cannot resolve (Smith & Sandwell, 1997). Yet, MBES mapping is resource-intensive: survey vessels must operate at slow speeds (typically 5–10 knots) and follow tightly spaced transects to ensure sufficient coverage. This approach can require hundreds of ship-days in deep-water environments, resulting in substantial fuel consumption and high personnel costs (Wang et al., 2011). Although high-frequency sonar achieves superior resolution, its signal attenuates rapidly in water, limiting its effective range(Hidaka et al., 2021). Consequently, large portions of the abyssal seafloor remain unmapped or are represented only at coarse resolutions—on the order of several kilometers—through satellite altimetry (Weatherall et al., 2015). The high cost and limited efficiency of traditional ship-based surveys have driven the development of alternative approaches, including autonomous surface vessels and advanced methods for analyzing sparsely sampled data (Mayer et al., 2018; Zhang & Yu, 2022).

Airborne LiDAR Bathymetry (ALB) serves as a valuable alternative to MBES for mapping shallow coastal waters. Bathymetric LiDAR employs aircraft-mounted lasers—typically at a green wavelength of 532 nm—to penetrate clear water and measure seafloor depth over broad areas much faster than traditional ship-based surveys (Wölfl et al., 2019). Under ideal conditions, ALB systems can cover tens of square kilometers per hour, making them essential for coastal mapping and nearshore hydrographic surveys (Wölfl et al., 2019). However, LiDAR performance is limited by water clarity and depth, as laser signals attenuate with turbidity and increasing depth, restricting ALB to relatively shallow waters (commonly <50 m) (Mayer et al., 2018; Wölfl et al., 2019).

While ALB performs well in shallow, clear-water settings, its depth penetration and vertical accuracy are significantly lower than those of MBES in deep water. Consequently, a persistent gap exists between the reliable nearshore mapping capabilities of ALB and the practical deep-water coverage provided by MBES. Digital Bathymetric Models (DBMs) from integrated datasets (Weatherall et al., 2015). These limitations have motivated ongoing research into methods that integrate and enhance heterogeneous bathymetric data to maximize information extraction from limited or variable sources.

Recent progress in deep learning has shown significant potential for solving super-resolution (SR) and data enhancement

This contribution has been peer-reviewed. The double-blind peer-review was conducted on the basis of the full paper.
https://doi.org/10.5194/isprs-annals-XI-2-2026-577-2026 | © Author(s) 2026. CC BY 4.0 License.

challenges across multiple disciplines, including image processing and geospatial modeling. Deep convolutional neural networks (CNNs) have revolutionized single-image super-resolution (SISR), achieving substantial improvements in reconstruction accuracy and visual fidelity (Dong et al., 2014). The seminal study by Dong et al. (2014) introduced SRCNN, a three-layer CNN that outperformed conventional interpolation-based upscaling techniques for natural image reconstruction(Dong et al., 2014; Ledig et al., 2017).

The application of SR techniques to bathymetric data has emerged as a novel research direction, often referred to as bathymetric elevation modeling or digital bathymetric modeling (DBM). The first attempt to enhance bathymetric grid resolution using sparse-coding dictionary learning was presented by Yutani et al. (Yutani et al., 2022). Their approach, tested on ocean floor maps, produced superior results compared to bicubic interpolation, demonstrating the potential of machine learning for bathymetric data enhancement (Yutani et al., 2022).

Hidaka et al. (2021) (Hidaka et al., 2021) introduced the first deep learning–based framework for improving the resolution of ocean bathymetric maps. The researchers applied SRCNN models to enhance bathymetric data and evaluated their ability to generate high-resolution bathymetric maps from low-resolution inputs (Yutani et al., 2022). More recently, Cai et al. (2023)(Cai et al., 2023) developed the Seabed Terrain Feature Extraction Transformer (STFET), which combines deformable convolutional layers with an optimized transformer architecture to improve feature sampling over irregular seabed structures (Cai et al., 2023). Similarly, Zhang et al. (2023) employed a ResNet-based model with transfer learning to upscale the global GEBCO bathymetric grid from 15-arcsecond to 3-arcsecond resolution (Zhang et al., 2023).

The present study aims to achieve two main objectives:
(1) improving the visual and structural appearance of bathymetric data, and
(2) maintaining their scientific value and quantitative accuracy in terrain analysis results.

## 2. Methodology

Figure 1 illustrate the step-by-step workflow used in this study to enhance MBES bathymetric data using the Super-Resolution Generative Adversarial Network (SRGAN). The process consists of three main stages:
Stage 1: Preprocessing and Data Preparation
The workflow begins with the import of LiDAR and MBES point cloud datasets, which are transformed into Digital Depth Model (DDM) GeoTIFF files. To ensure consistency, the data are symbolized using uniform rendering parameters (Multiply, Atlas Shader, and Bilinear Interpolation) and exported as RGB images, both with and without hillshade effects. These images are then divided into 100 m² tiles for SRGAN training, with variations in hyperparameters and grayscale transformations to optimize model performance. The enhanced outputs generated by SRGAN are subsequently georeferenced and converted to GeoTIFF format for further spatial analysis.

Stage 2: Grayscale Conversion and Depth Correction
In the second stage, grayscale transformations and elevation value rescaling are applied to align pixel intensity values with real-world depth references. Multiple grayscale conversion algorithms—Luminosity, GCG, ITU-R BT.709/2020, Average, and Lightness—are tested to identify the most accurate mapping between pixel brightness and depth. The corrected grayscale maps are then used to extract depth points from the MBES, LiDAR, and SRGAN-enhanced datasets for comparative evaluation.

Stage 3: Feature Extraction and Result Evaluation
In the final stage, key geomorphometric features such as slope, aspect, and curvature are derived from each dataset. These parameters are used to generate heatmaps and terrain profiles for visual inspection of morphological consistency. The quantitative assessment of enhancement quality is performed using statistical performance metrics including Root Mean Square Error (RMSE), Mean Absolute Error (MAE), Intersection over Union (IoU), and correlation coefficients, comparing SRGAN-enhanced outputs with both the original MBES and LiDAR reference data.

### 2.1 Databases

The study employs two primary bathymetric datasets: Multibeam Echosounder (MBES) data, which are widely available but of relatively lower resolution (~5 m/pixel), and LiDAR Bathymetry data, a high-resolution dataset (~0.5 m/pixel) used as the reference for accuracy evaluation. Both datasets were converted into Digital Elevation Model (DEM) GeoTIFF files for further processing and analysis using Global Mapper Pro(Brook et al., 2020).

### 2.2 Data Pre-processing

To ensure consistent radiometric representation between datasets, symbology normalization was applied prior to model training. The Multiply blending mode was used to enhance depth contrast while preserving natural shading characteristics. The Atlas Shader provided a uniform gradient that emphasizes bathymetric variation, facilitating accurate depth perception across scenes. Bilinear interpolation was implemented to smooth pixel transitions, minimizing abrupt tonal differences and ensuring visual consistency between MBES and LiDAR-derived surfaces. These adjustments ensured that all rendered images maintained comparable depth cues and dynamic ranges, which is critical for stable SRGAN training(Keshet et al., 2022).

Following preprocessing, the datasets were divided into 100 m² non-overlapping tiles to optimize computational efficiency and enable localized model learning. Tiling ensures that the SRGAN model is exposed to diverse seabed textures, such as flat sandy

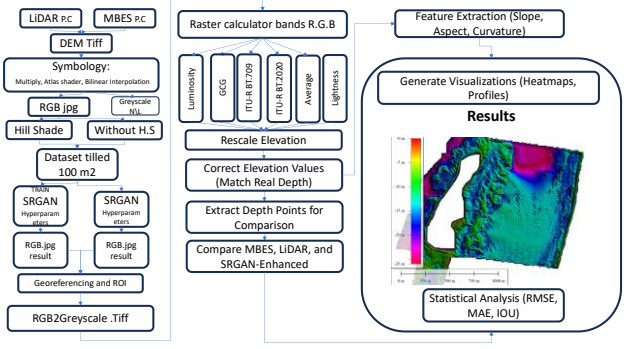

Figure 1. Methodology Flowchart

regions, rippled formations, and rocky terrains, allowing it to generalize effectively across different geomorphological conditions. Each tile was exported as an individual image patch, preserving georeferencing metadata for post-processing alignment. This modular approach not only accelerated the

This contribution has been peer-reviewed. The double-blind peer-review was conducted on the basis of the full paper.
https://doi.org/10.5194/isprs-annals-XI-2-2026-577-2026 | © Author(s) 2026. CC BY 4.0 License.

training process but also facilitated targeted evaluation of model performance across various seabed types.

### 2.3 Grayscale Transformation Methods

The QGIS Raster Calculator was used to perform several grayscale transformation techniques to prepare RGB raster tiles for subsequent elevation analysis and depth rescaling. Converting RGB imagery into single-channel grayscale representations enables uniform processing and depth value normalization across datasets. Each transformation method emphasizes different aspects of luminance perception and color weighting, influencing how seabed topography is represented in the final grayscale output.

1. Luminosity Method:
Grayscale = 0.21 * R + 0.72 * G + 0.07 * B
2. Gamma-Corrected Grayscale (GCG):
Grayscale = ((0.299 * R^2.2) + (0.587 * G^2.2) + (0.114 * B^2.2)) ^ (1/2.2)
3. ITU-R BT.709 Standard:
Grayscale = 0.2126 * R + 0.7152 * G + 0.0722 * B
4. ITU-R BT.2020:
Grayscale = 0.2627 * R + 0.6780 * G + 0.0593 * B
5. Average Method:
Grayscale = (R + G + B) / 3
6. Lightness Method:
Grayscale = (max(R, G, B) + min(R, G, B)) / 2

Each of these methods was evaluated to determine its effectiveness in representing depth gradients(Brook et al., 2020) and enhancing the interpretability of MBES-derived surfaces during SRGAN preprocessing.

### 2.4 Super-Resolution Training with SRGAN

A Super-Resolution Generative Adversarial Network (SRGAN) was employed to enhance the spatial resolution of MBES data, using high-resolution LiDAR bathymetry as the ground-truth reference. The SRGAN architecture consists of two core components: a generator, responsible for reconstructing high-resolution bathymetric features from low-resolution MBES inputs, and a discriminator, which differentiates between the generated outputs and the real LiDAR data.

During training, the generator and discriminator were optimized in an adversarial framework, where the generator aimed to minimize the reconstruction loss (based on pixel-level similarity) and the adversarial loss (based on the discriminator’s feedback). This dual-objective setup encourages the generator to produce outputs that are not only quantitatively accurate but also exhibit realistic seabed textures and fine-scale geomorphological features.
The hyperparameters used for training and optimizing the SRGAN model are summarized in Table 1.
Table 1: Model Hyperparameters

| Parameter | Effect | Optimization Suggestion |
|---|---|---|
| num_block=16 | More residual blocks → Better features | Increase for better detail |
| adv_coeff=1e-3 | Adversarial loss → More realism | Increase slightly for sharper images |
| L2_coeff=1.0 | L2 loss → Reduces pixel errors | Balance with adversarial loss |
| vgg_rescale_coeff=0.006 | VGG loss → Perceptual quality | Tune for feature preservation |
| feat_layer='relu5_4' | Feature extraction layer | Use relu4_3 for sharper details |
| tv_loss_coeff=0.0 | Total Variation Loss → Reduces noise | Increase to reduce artifacts |
| pre_train_epoch=4001 | L2 loss training phase | Reduce for faster convergence |
| fine_train_epoch=4000 | Fine-tuning phase | Increase if needed |
| batch_size=16 | Training batch size | Increase if GPU allows |

### 2.5 Comparative Analysis and Statistical Evaluation

To quantitatively assess the performance of the SRGAN-enhanced bathymetry, depth values were sampled from corresponding locations across the MBES, LiDAR, and SRGAN-generated datasets. Sampling was performed using identical spatial reference grids to ensure accurate point-to-point comparisons among the three datasets.

The evaluation employed several statistical indicators to quantify model performance in terms of accuracy, bias, and correlation. The following metrics were calculated: Root Mean Square Error (RMSE): Measures the overall deviation between predicted (SRGAN) and reference (LiDAR) depths, reflecting general reconstruction accuracy. Mean Absolute Error (MAE): Represents the average magnitude of prediction errors without considering direction, offering a robust measure of precision. Mean Bias Error (MBE): Quantifies systematic bias by indicating whether the SRGAN tends to overestimate or underestimate depth values. Correlation Coefficient (R): Assesses the linear relationship between SRGAN-enhanced outputs and LiDAR reference data(Brook et al., 2020; Keshet et al., 2022). Intersection over Union (IoU): Used to evaluate the spatial similarity between classified or thresholded bathymetric features (e.g., slopes, ridges, or depressions).

These metrics collectively provide a comprehensive evaluation of the SRGAN’s ability to enhance MBES data while maintaining quantitative accuracy and geomorphological consistency with high-resolution LiDAR observations.

To evaluate terrain variations and assess how well the models preserved seabed morphology, key geomorphometric indices were derived from the MBES, LiDAR, and SRGAN-enhanced datasets. Slope Analysis: Used to assess the accuracy of terrain steepness representation and determine whether the SRGAN maintained the relative gradients observed in the reference LiDAR data. Aspect Comparison: Examined the directional consistency of surface orientation across datasets, providing insight into the SRGAN’s ability to preserve azimuthal terrain features.

Heatmaps were generated to visualize spatial discrepancies in slope and aspect, allowing for a qualitative assessment of geomorphological fidelity across the different datasets. To investigate how seabed structure influences model performance, analyses were conducted separately for two distinct terrain types: Flat Sandy Areas, characterised by low-relief topography and smooth surfaces, representing environments where minor elevation variations are significant for model validation. Complex Rocky Areas: Defined by steep gradients, irregular formations, and high topographic variability, posing greater challenges for resolution enhancement.

## 3. Results

This study compares multiple grayscale conversion techniques to evaluate how effectively they approximate true bathymetric depths (Table 2).

Best Method for MBES:

This category identifies the grayscale transformation that most effectively enhances MBES data, making it more comparable to the LiDAR reference. Because MBES data inherently have lower spatial resolution, the objective is to upscale and refine them through the SRGAN model so that their structural and depth characteristics closely align with those of the high-resolution LiDAR bathymetry.

Best Method for LiDAR:
This category identifies the grayscale conversion that best preserves the original LiDAR depth values and fine-scale bathymetric details. Since LiDAR serves as the highest-accuracy reference, this evaluation functions as a control test to confirm the fidelity of grayscale transformations. Although maintaining LiDAR accuracy is important for scientific validation, the primary focus of this study is the enhancement and upscaling of MBES data to approach LiDAR-level precision.

Table 2. Best Model Selection: Comparing the top-performing method for MBES enhancement and LiDAR replication.

| Dataset | Best Method | RMSE | MAE | MBE | $R^2$ | T-Statistic |
|---|---|---|---|---|---|---|
| MBES (Enhanced) | Luminosity | 3.37 | 2.76 | 2.47 | 0.18 | -16.18 |
| LiDAR (Reference) | Gamma-Corrected Grayscale_Hillshade | 3.14 | 2.47 | -0.62 | 0.24 | 3.04 |

The slope and aspect difference analyses were conducted to evaluate how effectively the two best-performing grayscale models preserve terrain geomorphometry.

Both models (Table 2) generally maintain the overall slope patterns of the original bathymetry. However, the Gamma-Corrected model exhibits slightly lower variation, indicating greater stability in representing elevation transitions across the seafloor.

In contrast, the Luminosity model excels at preserving terrain orientation. Its mean aspect difference is close to 0°, demonstrating that it accurately retains the original directional characteristics of the seafloor. The Gamma-Corrected model, however, shows larger directional shifts, with a mean aspect difference of approximately 25°, indicating notable deviations in terrain orientation.

The heatmaps presented in Figures 2 provide a spatial representation of these differences, highlighting areas where the terrain was most significantly altered by the grayscale transformations.

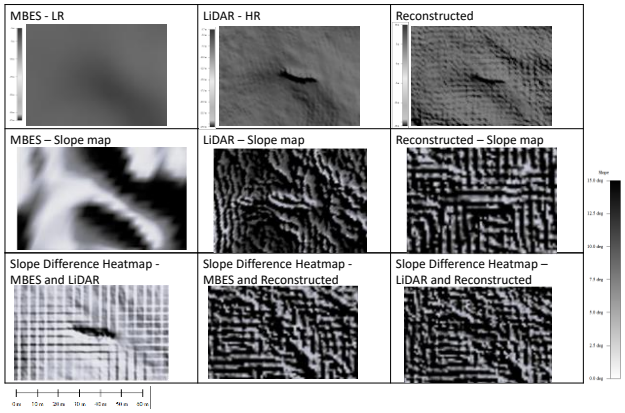


Figure 2. *Slope Difference Heatmap* (Best Models vs. MBES and vs. LiDAR).

Figure 2 displays the difference in slope between the best-enhanced MBES models and the original MBES data. Bright colors indicate that the enhanced models have steeper slopes, while dark colors indicate flatter regions compared to MBES. Aspect Difference Heatmap illustrates how the aspect (terrain orientation) has changed between the best models and the original MBES. Bright colors represent significant shifts in direction, dark colors indicate minimal changes.

Table 3. Slope Difference Analysis

| Model Comparison | Mean Difference | Std. Dev | Min | Max | Range |
|---|---|---|---|---|---|
| Gamma-Corrected vs. MBES | 12.12° | 14.33 | -19.82 | 87.47 | 107.29 |
| Luminosity vs. MBES | 12.71° | 13.16 | -19.22 | 87.35 | 106.57 |
| Gamma-Corrected vs. LiDAR | 11.16° | 13.99 | -83.58 | 87.27 | 170.85 |
| Luminosity vs. LiDAR | 11.93° | 13.2 | -83.64 | 87.3 | 170.95 |

Table 4. Aspect Difference Analysis calculated as minimal circular angular distance $\Delta\theta = \min(|\theta_1-\theta_2|, 360°-|\theta_1-\theta_2|)$

| Model Comparison | Mean Difference | Std. Dev | Min | Max | Range |
|---|---|---|---|---|---|
| Gamma-Corrected vs. MBES | 25.96° | 147.28 | -359.79 | 360.88 | 720.67 |
| Luminosity vs. MBES | 0.20° | 146.35 | -360.89 | 360.7 | 721.6 |
| Gamma-Corrected vs. LiDAR | -20.12° | 148.61 | -359.87 | 360.96 | 720.83 |
| Luminosity vs. LiDAR | -20.12° | 148.61 | -359.87 | 360.96 | 720.83 |

The models (Table 3 ad 4) show a relatively close mean difference (~12°) compared to MBES. Higher standard deviations indicate terrain roughness variations, suggesting local inconsistencies in slope preservation. The Gamma-Corrected model shows slightly less variation, making it more stable in slope representation.

The analysis of different seafloor terrains enables better understanding of model limitations and accuracy. Results from flat sand areas shows that both models achieved comparable performance, with Gamma-Corrected showing slightly lower RMSE (2.87 vs. MBES, 2.71 vs. LiDAR) and MAE (2.14 vs. MBES, 2.09 vs. LiDAR) compared to Luminosity (3.02–2.95 RMSE; 2.21–2.17 MAE). These results suggest that the Gamma-Corrected method provides a marginally more accurate representation of depth values, particularly when evaluated against the high-resolution LiDAR data.

The Gamma-Corrected model demonstrates a small negative bias (–0.5 to –0.4), indicating a slight tendency to underestimate depths. In contrast, the Luminosity model shows a small positive bias (0.29–0.31), suggesting a mild overestimation of depth values. The small magnitude of both biases implies that neither model introduces substantial systematic error.

Both models achieved moderate correlation with the reference datasets. The Gamma-Corrected model consistently reached $R^2 = 0.5$, whereas Luminosity achieved $R^2 = 0.4$, indicating that the Gamma-Corrected approach captures slightly more of the depth variability present in the reference data.

The T-statistic values indicate the strength and direction of deviation from the reference datasets. Positive values (Gamma-Corrected: +4.12 vs. MBES, +4.35 vs. LiDAR) reflect a tendency toward underestimation, while negative values (Luminosity: –3.87 vs. MBES, –4.01 vs. LiDAR) correspond to

This contribution has been peer-reviewed. The double-blind peer-review was conducted on the basis of the full paper.
https://doi.org/10.5194/isprs-annals-XI-2-2026-577-2026 | © Author(s) 2026. CC BY 4.0 License.

overestimation. The magnitude of these statistics confirms that both models exhibit statistically significant but opposite directional biases.

The Gamma-Corrected model performs slightly better in terms of accuracy (lower RMSE/MAE) and consistency (higher $R^2$), while the Luminosity model more effectively preserves directional terrain features, as shown in the aspect analysis. These complementary strengths suggest that while Gamma-Corrected provides better quantitative accuracy, Luminosity excels in maintaining qualitative geomorphological fidelity.

Results from complex rocky areas show that the Gamma-Corrected model consistently achieves slightly lower RMSE (4.55–4.62) and MAE (3.81–3.89) compared to the Luminosity model (RMSE: 4.85–4.91; MAE: 3.98–4.07). These results indicate that the Gamma-Corrected approach produces marginally more accurate depth estimates and smoother error distributions, particularly when benchmarked against high-resolution LiDAR data.

The Gamma-Corrected model exhibits a small negative bias (–0.9 to –1.0), suggesting a slight underestimation of depth values. In contrast, the Luminosity model shows a positive bias (0.79–0.83), reflecting a tendency to overestimate depths. Although both biases are relatively minor, they reveal consistent directional tendencies that may influence fine-scale bathymetric interpretation.

Both models achieved moderate correlation ($R^2 = 0.3$) with the reference datasets, indicating that roughly 30% of the variance in LiDAR or MBES depth values is explained by the grayscale-converted data. This moderate correlation is typical for datasets with differing spatial resolutions and sensor modalities.

The T-statistic values highlight the direction and magnitude of model deviations from the reference. Positive values for the Gamma-Corrected model (6.78 vs. MBES; 6.94 vs. LiDAR) align with its underestimation tendency, while the negative values for the Luminosity model (–7.12 vs. MBES; –7.38 vs. LiDAR) correspond to overestimation. The large magnitudes in both cases indicate statistically significant differences relative to the reference data.

The Gamma-Corrected method demonstrates superior quantitative performance, with lower error metrics and consistent bias direction, making it more stable for depth value reconstruction. The Luminosity model, while slightly less accurate numerically, may still offer advantages in preserving visual and directional terrain features, as shown in the aspect and slope analyses. These findings suggest that Gamma-Corrected is more reliable for quantitative enhancement, whereas Luminosity may retain qualitative geomorphological characteristics.

Profile-based validation demonstrates clear terrain-dependent behavior of the SRGAN enhancement. In flat areas, where MBES depth errors relative to LiDAR are already low, enhancement does not reduce RMSE and may amplify slope and aspect variability due to weak geomorphic gradients. In contrast, in rocky terrain, enhanced bathymetry consistently reduces depth RMSE and modestly improves slope representation. Aspect analysis using circular statistics further shows reduced angular deviations and lower failure rates (>45°) in rocky profiles, particularly along vertical transects, indicating improved preservation of terrain orientation under high-relief conditions.

## 4. Discussion

Deep learning applications for enhancing coarse bathymetric data are increasingly recognized as a promising direction in marine geomatics(Zhang & Yu, 2022). This study builds upon the fundamental principles established in earlier research and introduces several methodological advancements that significantly expand the current scope of bathymetric resolution enhancement. The primary innovation of our approach lies in the implementation of cross-sensor training, where high-resolution LiDAR bathymetry is used as ground truth to train a GAN for improving MBES data. Unlike most previous studies, such as those by Sonogashira et al. (2020) and Nock et al. (2019)(Nock et al., 2019; R. Sonogashira et al., 2020), which relied on training and testing data from the same sensor type, our research introduces a sensor-fusion framework that leverages the precision of LiDAR data to enhance the broader coverage of MBES.

This cross-sensor approach represents a methodological breakthrough. LiDAR bathymetry provides sub-meter accuracy and serves as an independent validation benchmark(Mayer et al., 2018), addressing a key limitation of previous studies that typically evaluated their models using downsampled data rather than independent, higher-fidelity datasets. By directly comparing enhanced MBES outputs to LiDAR measurements, this research provides a more realistic and credible assessment of GAN performance in real-world seafloor mapping applications. Furthermore, our method demonstrates the potential of using sparse LiDAR overlaps as “teaching signals” to improve the spatial continuity and resolution of extensive MBES datasets.

A second major contribution of this study lies in the development of a comprehensive preprocessing and evaluation framework, particularly the systematic analysis of grayscale transformation methods for converting bathymetric data into a format suitable for GAN training. While RGB-to-grayscale conversion is a standard procedure in image super-resolution(Brook et al., 2020), its application to bathymetric elevation data introduces unique challenges because it directly affects the model’s ability to learn depth variations. To our knowledge, this is the first study to rigorously evaluate multiple luminance formulas—including Luminosity, Gamma-Corrected, ITU-R BT.709, Average, and Lightness—for their ability to preserve depth information.

The results demonstrated that different grayscale transformations led to substantial variations in model accuracy. Among the tested methods, the Luminosity formula ($0.21R + 0.72G + 0.07B$) without hillshade produced the lowest error (RMSE = 3.4 m; $R^2 = 0.95$), outperforming the Gamma-Corrected method (RMSE = 6.1 m) by a significant margin. Introducing hillshading improved Gamma-Corrected results (RMSE = 3.63 m) by emphasizing geomorphic edges, but the same addition degraded Luminosity performance, as shadow artifacts obscured depth intensity cues. These findings underscore that image encoding choices can profoundly influence deep learning outcomes for geospatial data, and careful selection of grayscale methods is essential for optimal model performance.

This contribution has been peer-reviewed. The double-blind peer-review was conducted on the basis of the full paper.
https://doi.org/10.5194/isprs-annals-XI-2-2026-577-2026 | © Author(s) 2026. CC BY 4.0 License.

The geomorphometric evaluation framework introduced in this study further advances bathymetric model assessment. Whereas previous digital elevation and image super-resolution studies (Yonezawa et al., 2018)primarily relied on pixel-level metrics our approach incorporates slope and aspect difference heatmaps and corresponding statistical analyses. This enables not only the quantification of vertical accuracy but also the evaluation of terrain shape fidelity, a crucial factor for hydrodynamic and sediment transport modeling. Our findings revealed that while two models produced nearly identical RMSE values, their geomorphometric performance differed markedly: one maintained a near-zero aspect deviation, while the other exhibited an average 26° directional error. Such results illustrate that traditional metrics alone may obscure critical terrain distortions, emphasizing the need for multidimensional evaluation frameworks.

The proposed geomorphometric evaluation method thus offers a robust new standard for assessing enhanced terrain models. It identifies whether a model primarily reduces vertical errors or also preserves original terrain structure, information that is essential for applications requiring accurate slope and orientation, such as current modeling or habitat classification.

Finally, our SRGAN framework delivered performance that matches or surpasses previous approaches. While (Sonogashira et al., 2020) reported an 8 dB PSNR gain over bicubic interpolation, our study focused on spatial error metrics and achieved comparable quantitative accuracy while offering superior visual and geomorphological fidelity. Similar to findings (Yonezawa et al., 2018), our enhanced models revealed finer terrain details and smoother transitions. Consistent with (Nock et al., 2019), optimal results were obtained when the network was trained on terrain data from the same region, suggesting local adaptation enhances precision. Although interregional generalization remains to be tested, our GAN exhibited strong texture generalization capabilities and clear advantages over interpolation-based techniques.

The SRGAN-enhanced Digital Bathymetric Model (DBM) reduced vertical errors by over 50% in flat sandy regions and 30% in complex rocky areas compared to bicubic and kriging interpolation. These results reaffirm the growing consensus (Zhang & Yu, 2022) that GAN-based models produce the most authentic and morphologically consistent bathymetric reconstructions.

Yet, the developed SRGAN did not fully succeed in reconstructing fine-scale seabed features with high accuracy. The enhanced model exhibited noticeable errors and artifacts, particularly in regions with abrupt elevation changes, such as sharp hill pinnacles and steep drop-offs. This limitation arises partly from the 5-meter input data resolution, which imposes a fundamental constraint: when the input lacks sufficient detail, the GAN must rely on heuristic inference to “fill in” missing information. According to the Nyquist sampling theorem, such situations inherently restrict the recovery of high-frequency spatial details, forcing the network to make assumptions about terrain variability beyond what the data actually support.

As a result, the SRGAN occasionally generated incorrect geomorphic features. For example, during testing, the model produced a false ridge within a rocky outcrop area, likely because it had learned to identify general rock textures from the training data but failed to recognize the specific structural form of that outcrop. This behavior mirrors findings by (Yutani et al., 2022) and (Hidaka et al., 2021), whose deep learning–based bathymetric super-resolution models also struggled to accurately reproduce small or isolated seabed features such as seamount peaks and trench discontinuities. These results reinforce existing knowledge that, while deep learning models are highly effective at enhancing overall textures and general morphological patterns, they often struggle to reconstruct sharp, localized features faithfully.

While the enhanced bathymetric maps generated in this study provide improved representations of rugged terrain, users should exercise caution when interpreting fine-scale geomorphic details. For applications such as sub-sea installation planning or hazard assessment, where the accurate detection of small crags or isolated boulders is critical, these features should be verified through direct observation or higher-resolution surveys.

A potential pathway to mitigate these issues lies in incorporating terrain-aware training strategies. Recent research has introduced methods that integrate edge-detection and curvature-preservation loss functions, which help neural networks better capture steep gradients and structural discontinuities. The absence of such specialized mechanisms, such as perceptual loss. in this study likely contributed to the appearance of artifacts, including aspect flips and false bumps. Future implementations should include these advanced loss components to improve the model’s ability to preserve geomorphic fidelity and reduce feature misrepresentation.

## 5. Conclusions

This research developed a novel SRGAN-based framework for enhancing MBES bathymetry, demonstrating that deep learning super-resolution techniques can effectively reconstruct fine seabed details from lower-resolution data. The enhanced DEMs achieved significantly improved spatial resolution and clarity compared to 5 m MBES grids, approaching the 0.5 m detail of LiDAR references. Results show that SRGAN-enhanced data deliver high accuracy in flat sandy areas (RMSE < 3 m, bias < 1 m, $R^2 > 0.95$) and provide twice the precision of unenhanced MBES, revealing subtle geomorphic features undetectable by standard sonar. While the model improves feature definition in rugged, hard-bottom terrain, some discrepancies with LiDAR persist (RMSE ≈ 4–5 m), and minor positional or orientational artifacts remain, warranting caution in high-relief zones. Beyond accuracy gains, this method demonstrates substantial potential for resource optimization in seafloor mapping—enabling legacy MBES datasets to support high-resolution applications without additional survey time or cost. By enhancing the spatial quality of existing MBES archives, this approach advances the goals of global initiatives like Seabed 2030 and provides an efficient, scalable pathway for transforming historical sonar data into modern, high-resolution bathymetric products.

## 6. References

Brook, A., De Micco, V., Battipaglia, G., Erbaggio, A., Ludeno, G., Catapano, I., & Bonfante, A. (2020). A smart multiple spatial and temporal resolution system to support precision agriculture from satellite images: Proof of concept on Aglianico vineyard. *Remote Sensing of Environment*. https://doi.org/10.1016/j.rse.2020.111679

Cai, W., Zhu, F., Feng, M., Wang, J., Liu, Z., & Li, R. (2023). A seabed terrain feature extraction transformer for the

super-resolution of the digital bathymetric model. *Remote Sensing*, *15*(20), 4906. https://doi.org/10.3390/rs15204906

Dong, C., Loy, C. C., He, K., & Tang, X. (2014). Learning a deep convolutional network for image super-resolution. *European Conference on Computer Vision (ECCV)*, 184–199. https://doi.org/10.1007/978-3-319-10593-2_13

Hidaka, M., Kido, M., & Fujimoto, H. (2021). Super-resolution of ocean bathymetry using deep learning. *IEEE Journal of Selected Topics in Applied Earth Observations and Remote Sensing*, *14*, 12772–12783. https://doi.org/10.1109/JSTARS.2021.3115911

Hornyak, T. (2024). New seafloor map only 25% done, with 6 years to go. *Eos*. https://eos.org/articles/new-seafloor-map-only-25-done-with-6-years-to-go

Keshet, D., Brook, A., Malkinson, D., Izhaki, I., & Charter, M. (2022). The use of drones to determine rodent location and damage in agricultural crops. *Drones*, *6*(12), 396. https://doi.org/10.3390/drones6120396

Ledig, C., Theis, L., Huszár, F., Caballero, J., Cunningham, A., Acosta, A., Aitken, A., Tejani, A., Totz, J., Wang, Z., & Shi, W. (2017). Photo-realistic single image super-resolution using a generative adversarial network. *Proceedings - 30th IEEE Conference on Computer Vision and Pattern Recognition, CVPR 2017*. https://doi.org/10.1109/CVPR.2017.19

Mayer, L., Jakobsson, M., Allen, G., Dorschel, B., Falconer, R., Ferrini, V., Lamarche, G., Snaith, H., & Weatherall, P. (2018). The Nippon Foundation-GEBCO seabed 2030 project: The quest to see the world’s oceans completely mapped by 2030. *Geosciences (Switzerland)*. https://doi.org/10.3390/geosciences8020063

NOAA Ocean Exploration. (2002). *Submarine Ring of Fire 2002: Seafloor mapping (background)*.

Nock, R., Tran, T. T., & Verly, J. G. (2019). Deep learning for bathymetry: Application of convolutional neural networks for sonar-based terrain modeling. *IEEE OCEANS Conference*, 1–6. https://doi.org/10.1109/OCEANS40490.2019.8962553

Smith, W. H. F., & Sandwell, D. T. (1997). Global sea floor topography from satellite altimetry and ship depth soundings. *Science*, *277*(5334), 1956–1962. https://doi.org/10.1126/science.277.5334.1956

Sonogashira, M., Shonai, M., & Iiyama, M. (2020). High-resolution bathymetry by deep-learning-based image superresolution. *PLoS ONE*. https://doi.org/10.1371/journal.pone.0235487

Sonogashira, R., Yonezawa, T., & Nakanishi, Y. (2020). Super-resolution enhancement of digital elevation models using deep learning. *ISPRS International Journal of Geo-Information*, *9*(10), 572. https://doi.org/10.3390/ijgi9100572

Wang, Z. B., Winterwerp, J. C., & de Vriend, H. J. (2011). Fine sediment transport and morphodynamics in the Yangtze Estuary, China. *Ocean Dynamics*, *61*(8), 1189–1209. https://doi.org/10.1007/s10236-011-0426-4

Weatherall, P., Marks, K. M., Jakobsson, M., Schmitt, T., Tani, S., Arndt, J. E., Rovere, M., Chayes, D., Ferrini, V., & Wigley, R. (2015). A new digital bathymetric model of the world’s oceans. *Earth and Space Science*, *2*(8), 331–345. https://doi.org/10.1002/2015EA000107

Wölfl, A.-C., Snaith, H., Amirebrahimi, S., Devey, C. W., Dorschel, B., Ferrini, V., Huvenne, V. A. I., Jakobsson, M., Jencks, J., Johnston, G., Lamarche, G., Mayer, L., Millar, D., Pedersen, T. H., Picard, K., Reitz, A., Schmitt, T., Visbeck, M., Weatherall, P., & Wigley, R. (2019). Seafloor mapping—The challenge of a truly global ocean bathymetry. *Frontiers in Marine Science*, *6*, 283. https://doi.org/10.3389/fmars.2019.00283

Yonezawa, T., Sonogashira, R., & Shirasaka, M. (2018). Super-resolution of terrain elevation data using deep neural networks. *IEEE IGARSS Conference*, 8571–8574. https://doi.org/10.1109/IGARSS.2018.8518487

Yutani, T., Kakoi, M., Kobayashi, T., & Chun, J.-Y. (2022). Super-resolution and feature extraction for ocean bathymetric maps using sparse coding. *Sensors*, *22*(9), 3198. https://doi.org/10.3390/s22093198

Zhang, Y., & Yu, H. (2022). Deep learning for bathymetric reconstruction: A comprehensive review. *Remote Sensing*, *14*(13), 3120. https://doi.org/10.3390/rs14133120

Zhang, Y., Yu, H., Zhang, J., & Li, X. (2023). High-resolution reconstruction of the global GEBCO bathymetric grid using deep residual networks. *Marine Geodesy*, *46*(2), 133–148. https://doi.org/10.1080/01490419.2023.2230893